Alkali-cellulose/ Polyvinyl alcohol biofilms fabricated with essential clove oil as a novel scented antimicrobial packaging material

Asmaa Sayed , Gehan Safwat , Manar Abdel-raouf ,
Ghada A. Mahmoud

PII: S2666-8939(22)00088-3
DOI: https://doi.org/10.1016/j.carpta.2022.100273
Reference: CARPTA 100273

To appear in: *Carbohydrate Polymer Technologies and Applications*

Received date: 3 November 2022
Revised date: 23 November 2022
Accepted date: 4 December 2022

Alkali-cellulose/ Polyvinyl alcohol biofilms fabricated with essential clove oil as a novel scented antimicrobial packaging material

Asmaa Sayed[1], Gehan Safwat[2], Manar Abdel-raouf *[3] and Ghada A. Mahmoud[1]

[1]Polymer Chemistry Department, National Center for Radiation Research and Technology, Egyptian Atomic Energy Authority, Cairo, Egypt.
[2]Faculty of Biotechnology, October University for Modern Sciences and Arts (MSA) Egypt.
[3]Egyptian Petroleum Research Institute, 1Ahmed Elzomor Street, 11727, Nasr city, Cairo, Egypt

*Email corresponding author: drmanar770@yahoo.com

Abstract:
The increased environmental awareness issues encouraged the manufacture of food -wares and packaging items from cellulosic materials to cope with the rapid growth of fast- food industry. In this work, scented biofilms with potent antimicrobial activity were prepared in a multi-step process assisted with the AFM. The biofilms comprised of polyvinyl alcohol (PVA) physically crosslinked with different weight ratios of alkaline cellulose (Na-Cell) [PVA/Na-Cell]. Then, the effect of gamma irradiation on the surface features of the optimized sample (PVA/Na-$Cell_4$) was verified at 5-25 KGy. The optimum film (PVA/Na-$Cell_4$.20kGy) was fabricated with different weight ratios of essential clove oil (ECO). The biofilms were characterized by the AFM, FT-IR, XRD, TGA, and the DMA. The contact angle measurements of the optimized films reveal wettability resistance as following: PVA/Na-$Cell_4$.0kGy (102.48^o) < PVA/Na-$Cell_4$.20kGy (133.66^o)< PVA/Na-$Cell_4$.ECO20kGy (140.62^o). The antimicrobial investigation displayed remarkable effect against different pathogens. Therefore, the claimed biofilms are excellent candidates for packaging application.

Keywords:

Alkaline cellulose, Polyvinyl alcohol, Atomic force microscopy, clove oil, green packaging, antimicrobial activity.

1. Introduction:

Active packaging is an emerging technology -compared with traditional “inert packaging”- involves incorporation of active components such as oxygen scavengers, antioxidants, and antimicrobial agents (Das, Ringu, Ghosh, & Pramanik, 2022; Kuai et al., 2021). Active packaging can be classified according to the type of the additive added into the film as chemo-active or bioactive. Chemo-active packaging affects the chemical composition of the food product and the gaseous atmosphere inside the pack. While bioactive packaging contains antioxidant and antimicrobial agents that interact with biological molecules and may prevent the growth of different microorganisms (Sharma, Barkauskaite, Duffy, Jaiswal, & Jaiswal, 2020). In this context, Essential oils are natural plant byproducts with antioxidant, antimicrobial, or antifungal properties (Luesuwan, Naradisorn, Shiekh, Rachtanapun, & Tongdeesoontorn, 2021).

They include many nice pungent scented species such as mint oil, cinnamon oil, and clove oil. The latter is extracted from the aromatic flower buds of a tree in the family Myrtaceae, *Syzygium aromaticum*. It contains a number of bioactive compounds, including Eugenol, which has potent insecticidal, antioxidant, and antifungal properties (Mulla et al., 2017).

On the other hand, employment of green polymers to substitute fossil-based polymers in diverse applications has attracted much attention (Sayed, Mahmoud, Said, & Diab, 2022). In this regard, carbohydrate polymers such as cellulose and chitosan are gaining much interests as promising building blocks for the production of benign active packaging films because of their biodegradability, biocompatibility, renewability, beneficial film-forming performance, and ease of accessibility **(**Azman, 2022**;** Baranwal, Barse, Fais, Delogu, & Kumar, 2022**)**. These polymers must be chemically adapted to improve their properties to fit packaging application. Water resistance is one of the major criteria that judges the film applicability because moisture is one of the most detrimental factors that affects food (Helanto, Matikainen, Talja, & Rojas, 2019; Schoukens et al., 2014). Higher values for water solubility at ambient temperature have been observed for films containing green polymers (Stadler & García-Peñas, 2022). Cellulose is the most abundant high functional hydrophilic polymers (Tajeddin, 2014). Although the high film forming property of cellulose, its poor mechanical properties limit its employment in packaging application. However, modification of cellulose into packaging application has been investigated. In this regard, bio-nanocomposite films composed of poly (butylene adipate-co-terephthalate) (PBAT), poly (lactic acid) (PLA) PBAT/PLA and cellulose nanocrystals (CNCs) extracted from agrowaste were investigated (Andrade et al., 2022). Furthermore, Arrieta et al (Arrieta et al., 2014) applied the cellulose nanocrystals (CNCs) obtained from the acid hydrolysis of microcrystalline cellulose to improve the mechanical properties of poly(lactic acid)–poly(hydroxybutyrate) (PLA–PHB) blends. In addition, cellulose nanocrystals were used to modify the mechanical properties of Poly(vinyl alcohol) (El Miri et al., 2016). However, chemical treatment of pristine cellulose with chemical agents yielded modified cellulose with desirable mechanical properties for use as a packaging material (Boufi et al., 2016; Liu et al., 2021). Tu et al (Tu et al., 2022) reviewed alkali/urea aqueous system as one of the green cellulose solvents fulfills the features to be used for low-cost and strong efficient preparation of regenerated cellulose fibers. In addition, Xia et al developed novel multi-functional cellulose/ tea polyphenols (TPs) bio-hybrid films with high anti-ultraviolet activity and irradiation stability (Xia, Ji, Xu, & Ji, 2022). The existence of phenolic hydroxyls afforded the films with high bacterial activity. In another work, cellulose was treated NaOH to yield Alkali-cellulose with enhanced mechanical properties (Yuvaraj et al., 2021).

On the other hand, Polyvinyl alcohol is one of the semi-crystalline non-toxic synthetic polymers whose backbone consists of zigzag shape carbon chains. Due to it reasonable mechanical properties and film forming readiness, it is most commonly used for food packaging (Suganthi, Vignesh, Kalyana Sundar, & Raj, 2020). Bahrami and Fattahi prepared biodegradable films comprised of carboxymethyl cellulose and polyvinyl alcohol fabricated with an essential oil and investigated their physicochemical properties (Bahrami & Fattahi, 2021).

Generally, films are crosslinked architects, which can be made either by physical or chemical crosslinking. Chemical crosslinking can be achieved by many protocols (Campiglio et al., 2020; Mane, Ponrathnam, & Chavan, 2015). Gamma irradiation is one of the most favorable crosslinking induced means due to its greenness, readiness and flexible applicability (Al-Qudaha, Hegazyb, Mahmoudb, & Hegazyb, 2022; Sayed, Hany, Abdel-Raouf, & Mahmoud, 2022; Sayed, Mohamed, Abdel-raouf, & Mahmoud, 2022).

The main hypothesis in the current work is introducing green biodegradable films with potent antimicrobial properties based on alkaline cellulose in a multi-step protocol guided by the AFM outcomes. Initially, the claimed films comprised of physically crosslinked alkaline cellulose and polyvinyl alcohol PVA/Na-Cell. The variation in surface features of these composites due to the change in alkaline cellulose content was investigated via the AFM for their topography and roughness. Then, the optimized sample was exposed to different irradiation doses in order to verify the effect of gamma irradiation on the surface topography and the mechanical properties of the prepared films. At last, the film with optimum features is fabricated with different weight percentages of essential clove oil to induce the antimicrobial effect. The prepared films were characterized with the FTIR, TGA, and XRD while their hydrophobicity was assured via contact angle measurement. The mechanical properties of the optimized films were also investigated. Moreover, the antimicrobial activity of the fabricated optimized membrane was verified.

2. Materials & Methods

2.1. Materials

Cellulose (Cell.) microcrystalline powder (average Mwt 90 x 10^3) was purchased from PubChem CID. Polyvinyl alcohol (PVA) [Mwt = 115,000 kDa, Degree of hydrolysis: 85-90%] was purchased from OXFORD laboratory reagent, (India). NaOH was supplied from ALPHA CHEMIKA, Mumbai (India) as white pure flakes. Other chemicals, such as solvents and glycerol were supplied from El-Nasr Co. for Chemical Industries, Egypt. Clove (*Syzygium aromaticum*) buds were purchased from traditional and folk medicine plants store in Cairo- Egypt and authenticated in the Department of Botany, Faculty of Agriculture, Cairo-Egypt.

2.2. Alkaline treatment of cellulose (Na-Cell.)

Shortly, 10g of cellulose powder was dispersed in 100mL alkaline solution (4%NaOH) with continuous stirring for 4h at 60^{o}C. Then the obtained alkaline cellulose powder was filtrated and washed several times until pH reaches 7.0. Afterwards, the Na-Cell was dried in an oven at 50^{o}C.

2.3. Extraction of essential clove oil:

The hydro-distillation technique was used to extract the essential clove oil ECO. Briefly, 50g of Clove seeds were crushed and dissolved in 500mL of 10% NaCl saline solution. The mixture was then placed in a Clevenger-type apparatus for 4 hours, as described by the British Pharmacopoeia. The recovered essential oil ECO was dried over anhydrous sodium sulphate. The purified ECO was stored in a dark glass vial at 4–8 °C, for future use (Nada, Mohsen, Zaki, & Aly, 2022).

2.4. Preparation of PVA/ Na-Cell. films

A facile methodology was used to create the green cellulose based reinforced films. Simply, the desired weight of PVA was dissolved in distilled water before adding the defined amount of Na-Cell as shown in Table 1. The mixture was stirred until homogeneity was attained. Then a mix of citric acid and glycerol is added with continuous stirring for 2 hours. Next, 15ml of the resulting solutions were poured into polystyrene petri dishes (10cm) and dried in an oven at 40°C for 24 hours. The films were investigated by the AFM and the optimum biofilm was irradiated with gamma rays from a ^{60}Co gamma cell irradiator at different irradiation doses of 5, 10, 15, 20, and 25 kGy and at dose rate of 1.66 kG/h. The irradiated composites were poured into polystyrene petri dishes (10cm) and dried in an oven at 40°C for 24 hours. Finally, the films were removed and stored at room temperature in polyethylene bags.

2.5.Fabrication of the green films with clove oil:

The optimum sample was selected by the aid of the AFM outcomes (PVA/Na-Cell$_4$). Then the previous steps were repeated to the optimized formulation and irradiated at an irradiation dose of 20 kGy. Different concentrations of ECO (0, 25, 50, 75, and 100µml) were added to 15 mL of the irradiated composite separately and stirred for an hour. Then, the PVA/Na-Cell$_4$/ECO composites were poured on polystyrene Petri dishes (10 cm) and dried in an oven at 40°C for 24 hours. Finally, the films were gently removed and stored at room temperature in polyethylene bags.

Table 1: Codes of PVA/Na-Cell

Code	PVA(g)	Na-Cell. (g)	Citric acid (g)	Glycerol (mL)	Dis H_2O (mL)
PVA/Na-Cell$_0$	5.0	0.0	1.0	1.5	100
PVA/Na-Cell$_1$	4.5	0.5	1.0	1.5	100
PVA/Na-Cell$_2$	4.0	1.0	1.0	1.5	100
PVA/Na-Cell$_3$	3.5	1.5	1.0	1.5	100
PVA/Na-Cell$_4$	3.0	2.0	1.0	1.5	100
PVA/Na-Cell$_5$	2.5	2.5	1.0	1.5	100

2.6. Instrumental analysis and characterization:

- The topography, height, and roughness of the prepared membranes were examined using the AFM, Flexaxiom Nanosurf, C3000 in dynamic mode (non-contact) at room temperature. The AFM imaging was performed with an NCLR rectangular-shaped silicon cantilever with a resonant frequency of 9 kHz.
- The FT-IR spectra of the optimized films were recorded between 4000 and 400 cm^{-1}, with a resolution of 4 cm^{-1}, using a Bruker Vertex.70 FT-IR spectrometer.
- The crystallographic properties of the optimized films were investigated at room temperature using a Shimadzu Diffractometer D6000 (30 mA and 40 kV) at Cu K (=1.54) radiation in a 2 range of 4-90 scan speed 8°/min.

- The thermogravimetric analysis (TGA) was carried out on a TGA-30 (Shimadzu, Japan) at a heating rate of 10 °C/min in a nitrogen atmosphere over a temperature range of room temperature to 600 °C.
- The mechanical properties of nanocomposite films were measured using Hounsfield tensile testing equipment (model H10 KS) on Dumbbell-shaped specimens of 50mm length and 4mm neck width at room temperature. The films were driven at 10 mm/min, and the analyses were performed with a 20 kN load cell.
- VCA Video Contact Angle System, Kr ÜssDSA25B, Germany, was used to measure contact angles. The contact angle between the water and the film was measured at room temperature by placing a water drop onto the film surface with a digital micro syringe.

2.7. Antimicrobial activity

The antimicrobial activity of the prepared membranes was evaluated using the agar well-diffusion method. Spreading a volume of the microbial inoculum over the entire agar surface inoculates the agar plate surface. Then, using a sterile cork borer or tip, a hole with a diameter of 6 to 8 mm was punched aseptically, and a 5mm diameter circular piece of the desired membrane was placed in each hole. The agar plates are then incubated under appropriate conditions based on the test microorganism (Magaldi et al., 2004). Following incubation times of 16 to 24 h (*Mucoraceae*) and 24 h (*A. fumigatus*, *A. flavus*, *A. niger*), the diameters of the inhibition zones (in mm) surrounding the wells were measured to the nearest whole millimetre at the point where there is a noticeable reduction in growth.

2.8. Statistical analysis

For each film, at least three measurements were taken at different locations to ensure accuracy in estimation of the contact angle and AFM data. Also, the mechanical properties were performed five replicates for each treatment. The data were plotted using Origin 2018(Origin Lab Corp., Northampton, MA01060, USA), and all the results were statistically analyzed using the ONE-WAY ANOVA. Differences among average values were analyzed by Duncan's multiple range tests using IBM SPSS software version 24 as a statistical resource at $P < 0.05$.

3. Results and discussion:

3.1.AFM characterization:

In this study, green films were prepared through a multi-step protocol guided with the AFM data. The first step involved preparation of cellulose-based biocomposite films via physical crosslinking between polyvinyl alcohol and alkaline cellulose in presence of glycerol and citric acids as plasticizer and crosslinker, respectively. The surface morphology and surface roughness of the claimed membranes were verified via the AFM. The AFM is extensively used throughout this work to verify the effect of different factors on the features of the prepared films on the bases of their height and surface roughness (Sayed, Yasser, Abdel-raouf, & Mohsen, 2022). It is used also to select the optimized sample at each stage of the work. AFM characterization was achieved by dynamic mode to inspect three AFM outputs:

- The topography of the sample,
- The height expressed by the Z-axis to define the difference between the maximum point above the surface and the minimum point below the surface and,

● The roughness measurements to monitor Phyisco-chemical changes that occurred to the investigated samples.

Based on previous studies (Chu et al., 2019; Nisar et al., 2018), the height and the thickness measurements of the films are influenced by the compatibility between polymer and filler, the number of solid contents, and the free volumes inside the film matrix.

3.1.1. Effect of alkaline cellulose content on the surface features of PVA/NaCell films

Figure 1A displays the AFM image of the alkaline cellulose which reveals crystalline surface with very tiny protrusions. Moreover, Figure1(B-G) depicts the surface topography of PVA/Na-Cell$_{0-5}$, and Table 2A tabulates the AFM data extracted from the images. It can be seen that the PVA/Na-Cell$_0$, which is comprised merely of PVA, has the lowest height and roughness and the AFM image demonstrates minute masses of PVA. The addition of Na-cellulose to PVA/Na-Cell$_1$, PVA/Na-Cell$_2$, and PVA/Na-Cell$_3$ gradually changes the surface appearance into a smoother and slightly raises the roughness measurements. On the other hand, a dramatic decrease in the height measurement was observed in images f and g, which are assigned for PVA/Na-Cell$_4$ and PVA/Na-Cell$_5$, respectively. The height bars for these two films showed that the measuring unit is a picometer, indicating complete dispersion of Na-Cell in the PVA matrix. The smooth surfaces confirmed the even distribution of Na-Cell internally. The increase of Na-Cell content in PVA/Na-Cell$_5$ causes increasing in the height and decreasing the roughness values compared to PVA/Na-Cell$_4$. Therefore, PVA/Na-Cell$_4$ was selected as the optimized sample of this stage.

3.1.2. Effect of irradiation dose on surface feature of PVA/Na-Cell$_4$

Although the gamma irradiation is among the green protocols for crosslinking, the higher doses may cause extremely crosslinked rigid structure with inferior mechanical properties such as brittleness, very low elasticity modulus, very narrow pores, and high surface roughness. Therefore, the effect of irradiation dose induced crosslinking on the topography of PVA/Na-Cell$_4$ was monitored as shown in Figure 2 (A-E). In this regard, five irradiation doses were applied: 5, 10, 15, 20 and 25 kGy. As illustrated in Table (2A), the height measurement increases in accordance to the irradiation dose. This could be attributed to the emergence of more crosslinking spots. It is be noted that some striations are shown in some images Figure 2 (C-E) which are probably caused by highly crosslinked masses formed as a result of the irradiation effect. Based on the height and roughness measurements, PVA/Na-Cell$_4$ (20kGy) is expected to achieve the best performance as a packing film with moderate height and roughness.

3.1.3. Effect of essential clove oil on the surface features of the fabricated sample

Figure 2F shows AFM image of the PVA/Na-Cell$_4$ sample with essential clove oil at irradiation dose of 20kGy, and the AFM outcomes are also tabulated in Table 2A. The increase in height and decrease in roughness measurements indicated that the oil formed a layer onto the surface of the biofilm appears in the form of tiny protrusions. Our data is consistent with Bahrami and Farrahi findings who observed that the thickness of the biofilm comprised of carboxymethyl cellulose/ Poly vinyl alcohol gradually increased by the addition of the essential oil which confirms that the oil formed a layer over the film's surface and it is not impregnated within the film matrix (Bahrami & Fattahi, 2021). In addition, the images are analyzed by a special software to display the layer of clove oil that cover the biofilm (Figure 3A) and the phases comprising the biofilm (Figure 3B).

Table 2A: AFM data of PVA/Na-Cell versus Na-Cell content, irradiation dose and the ECO

Sample	Roughness Ra (nm)	Height
PVA/Na-$Cell_0$	$3.88^{c} \pm 0.11$	$1.11^{e} \pm 0.01$ nm
PVA/Na-$Cell_1$	$4.02^{c} \pm 0.23$	$1.33^{e} \pm 0.03$ nm
PVA/Na-$Cell_2$	$4.34^{d,e} \pm 0.21$	$2.65^{e} \pm 0.06$ nm
PVA/Na-$Cell_3$	$4.82^{e,f} \pm 0.19$	$3.08^{e} \pm 0.07$ nm
PVA/Na-$Cell_4$	$1.11^{a} \pm 0.08$	$260^{a} \pm 2.09$ pm
PVA/Na-$Cell_5$	$2.14^{b} \pm 0.07$	$670^{b} \pm 6.24$ pm
PVA/Na-$Cell_4$,5kGy	$1.08^{a} \pm 0.09$	$1.27^{e} \pm 0.01$ nm
PVA/Na-$Cell_4$,10kGy	$3.45^{c} \pm 0.11$	$1.15^{e} \pm 0.01$ nm
PVA/Na-$Cell_4$,15kGy	$5.14^{f} \pm 0.19$	$1.60^{e} \pm 0.04$ nm
PVA/Na-$Cell_4$,20kGy	$5.24^{f} \pm 0.19$	$816^{c} \pm 4.32$ pm
PVA/Na-$Cell_4$./ECO.20 kGy	$19.10^{h} \pm 1.07$	$12.4^{f} \pm 2.91$ nm
PVA/Na-$Cell_4$,25kGy	$9.15^{g} \pm 0.46$	$830^{d} \pm 5.20$ pm

The values are the means ± SD, n=3 inside each column with different letters are significantly different at $P<0.05$, Duncan's test.

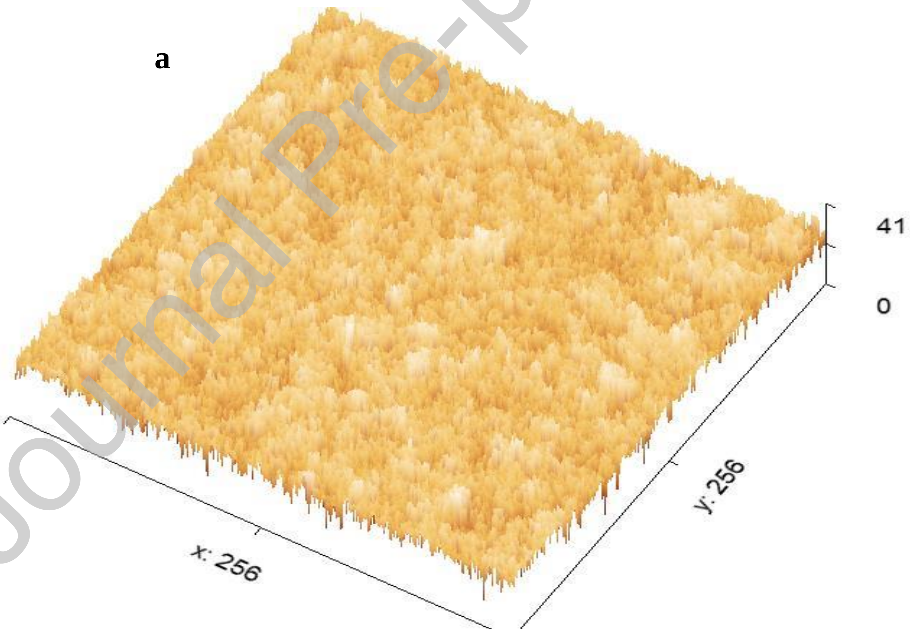

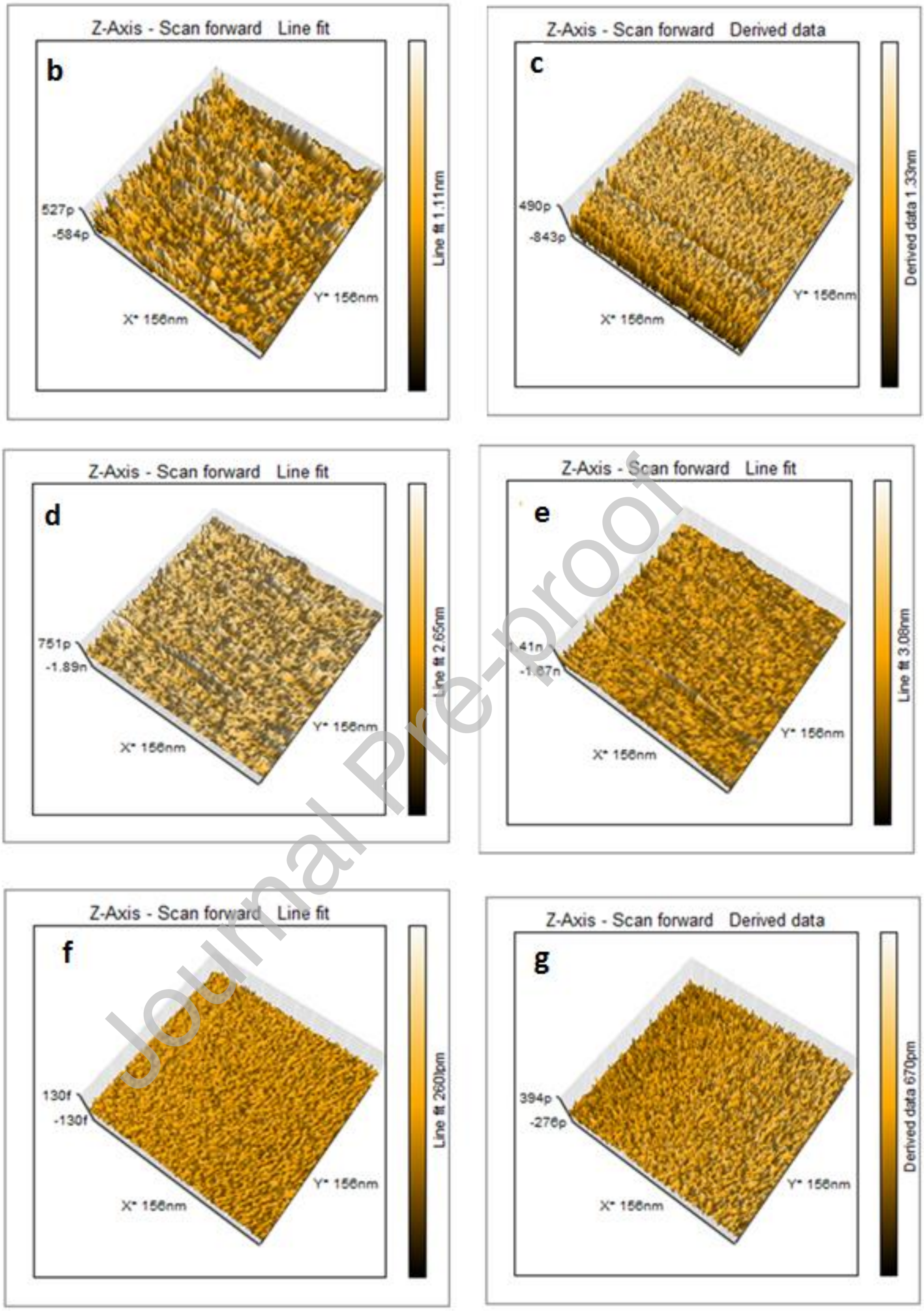

Figure 1: The AFM images of PVA/Na-Cell as a function of Na-Cell content (A) alkaline cellulose, (B) PVA/Na-$Cell_0$, (C) PVA/Na-$Cell_1$, (D) PVA/Na-$Cell_2$, (E) PVA/Na-$Cell_3$, (F) PVA/Na-$Cell_4$ and

(G) PVA/Na-Cell5.

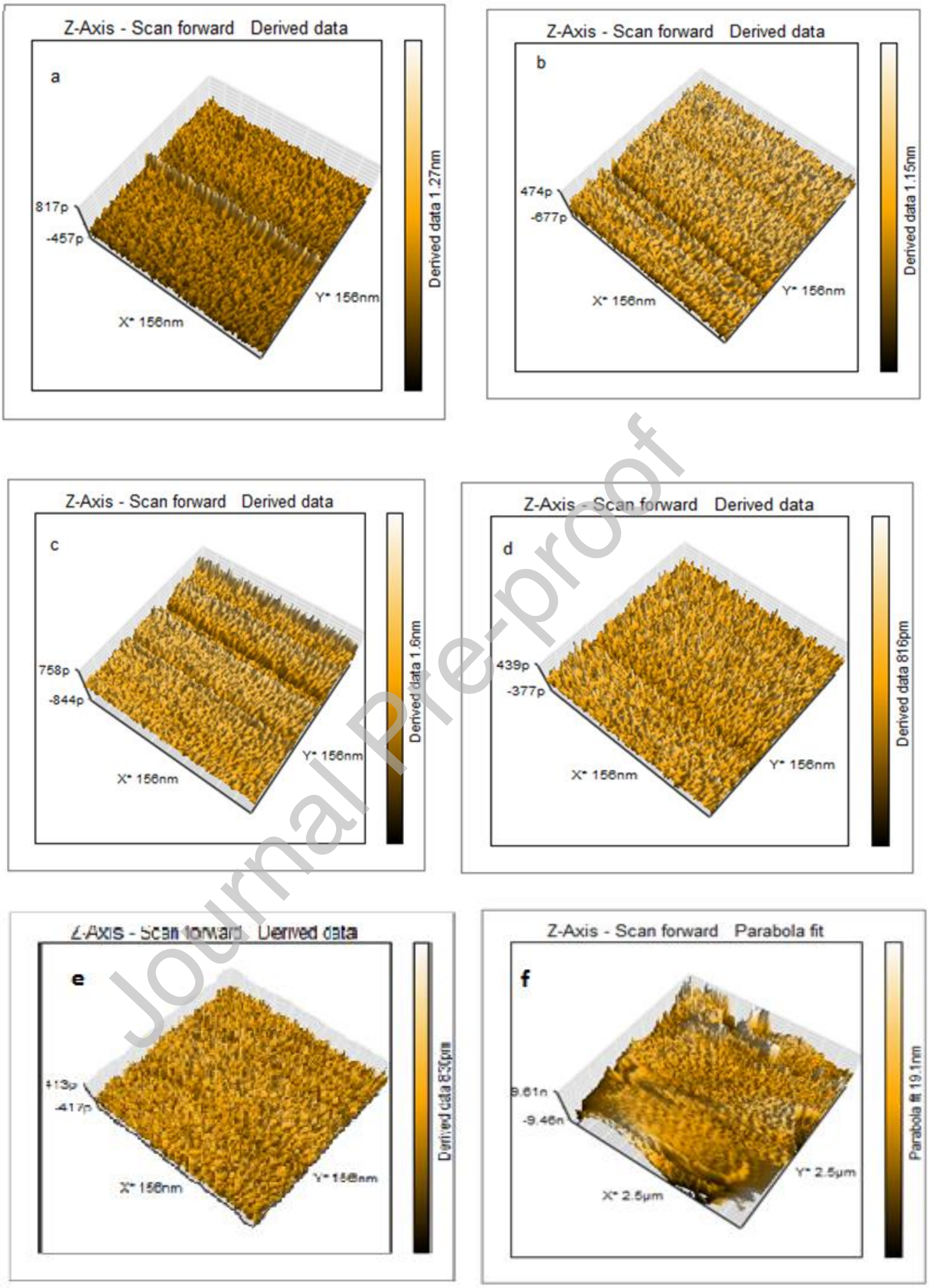

Figure 2: The AFM images of PVA/Nacell$_4$ as a function irradiation dose (kGy) and clove oil; (A) 5kGy (B) 10kGy, (C) 15kGy, (D) 20kGy and (E) 25 kGy and (F) with ECO.

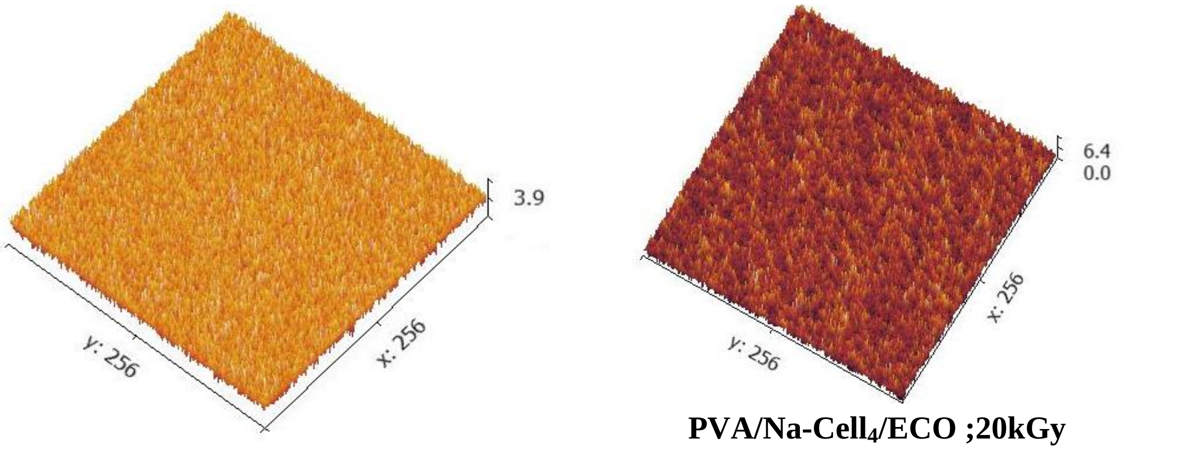

PVA/Na-Cell$_4$;20kGy **PVA/Na-Cell$_4$/ECO ;20kGy**

Figure 3A: Gwyddion analysis of PVA/Na-Cell$_4$.20kGy and PVA/Na-Cell$_4$./ECO 20kGy

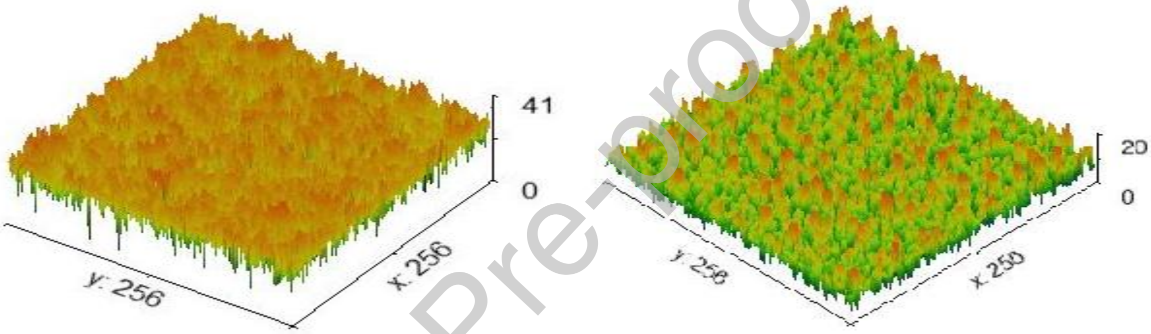

Two-phase image of PVA/Na-Cell$_4$ 20kGy **Three-phase image of PVA/Na-Cell$_4$/ECO 20kGy**

Figure 3B: Phases of the biofilm composites

3.2. Infrared spectroscopy (FTIR)

The proposed mechanism for the biofilm formation is given in Figure 4A. The chemical structure of PVA, Na-Cell, PVA/Na-Cell$_4$.0kGy, PVA/Na-Cell$_4$.20kGy, and PVA/Na-Cell$_4$/ECO 20kGy films was verified using FTIR analysis to track the disappearance of definite peaks or the appearance of new ones, as shown in Figure 4B. The spectrum of PVA depicts all of the major peaks related to hydroxyl and acetate groups. The stretching vibration of O-H of PVA is responsible for the wide band observed between 3550 and 3200 cm^{-1}. The vibrational band observed between 3000 and 2840 cm^{-1} refers to the stretching vibration of C–H from alkyl groups and the peaks between 1750–1735 cm^{-1} are assigned to the stretching vibration of C=O from the acetate group remaining from PVA. The stretching vibration band at 1027 cm^{-1} is due to C-O (Al-qudah, Mahmoud, & Abdel Khalek, 2014). In the spectrum of PVA/Na-Cell$_4$.0kGy, there is a considerable reduction of the intensities of the O–H, C=O, and C-O peaks indicating the interaction between PVA and Na-Cell as a possible formation of acetal bridges. A shift in peak positions was also observed, with the stretching vibration of the carbonyl group validated to 1720-1740 cm^{-1} and the O-H stretching vibration peak verified to 3330-3350 cm^{-1}. Irradiation caused only a minor change in the sample for PVA/Na-$Cell_4$.20kGy when compared to the unirradiated one. Irradiation caused a broadening of the intensity of the O-H peak and splitting of the C-O peak by the effect of gamma induced-crosslinking. The incorporation of ECO into the matrix of PVA/Na-$Cell_4$/ECO.20kGy appears as a fingerprint at 607 cm^{-1}.

3.3. Thermal analysis

Thermal stability of polymer composites is one of the most important properties that directs the application of a designed formulation in a specific application. TGA is used to evaluate materials thermal stability and the percentage of volatile components by monitoring the weight loss of the sample in an inert atmosphere as a function of temperature. Figure 4C shows the TGA/DTG thermograms of PVA, PVA/Na-$Cell_4$;0kGy and irradiated PVA/Na-$Cell_4$;20kGy. The samples were measured in the temperature range from 30^{o}C to 600^{o}C with a constant rate of 20^{o}C/min under nitrogen atmosphere. The TGA and DTG curves show that all samples exhibited three distinct weight loss stages. The same pattern was found by Othman et. al., in their study on the thermal properties of polyvinyl alcohol and corn starch films (Othman, Azahari, & Ismail, 2011). In the thermogram of PVA, the first stage presents the evaporation of the partially physically sorbed water while the second stage displays the disintegration of side chain of PVA. The third stage shows the decomposition of main chain of PVOH. The data in Table 2B expresses that the major weight loss is detected at about 80-100 wt% in the range of 200-400ºC for the PVA sample which inters complete decomposition. On the other hand, physically crosslinked PVA-alkaline cellulose displayed better degradation profile with higher thermal stability with about 18% mass left at 600^{o}C. This may be attributed to the crystalline nature of cellulose which affords higher thermal stability. Our data are opposite to Othman et al findings who reported that the pure PVA displayed higher thermal stability than that of PVOH/corn starch composites due to the different nature of starch than cellulose. The first-order derivative of TGA curves disclose the temperature at which the maximum decrease of mass takes place. It is clearly shown that the side chains of PVA are readily decomposed at 100^{o}C prior to the main chains (356 ^{o}C) and achieved complete degradation at 437 ^{o}C. On the other hand, the maximum weight loss of the PVA/ alkaline cellulose (physically and chemically crosslinked) shifted to a higher temperature compared to pure PVA. Recalling the data of the decomposition stages (Table 2B), the percentage weight loss at 356^{o}C and 600^{o}C for the pure PVA and the PVA/Alkaline cellulose blended film are shifted to lower mass loss due to the incorporation of the alkaline cellulose. However, the irradiated film depicted higher thermal stability than the physically crosslinked film. This may be attributed to that crosslinking with alkaline cellulose generated more intermolecular bonding and additional crosslinking points (Miranda et al., 2015; Nordin, Othman, Kadir, & Rashid, 2018). The data also reveals that the amount of bounded water represents only 1-4% of the irradiated biofilm which reflects its high-water resistance which is extremely required in packaging material. Based on the thermal profile of the biofilms, it can be concluded that PVA/Na-$Cell_4$; 20kGy is a proper green packaging candidate.

3.4. XRD analysis

The crystallinity is one of the major factors that judge the applicability of the membrane material. The effect of structure variation on the crystallinity of the prepared films was investigated by comparing the XRD patterns of PVA, PVA/Na-$Cell_4$;0kGy and PVA/Na-$Cell_4$; 20kGy, Figure 4D. The XRD pattern of the pure PVA membranes displayed strong crystalline reflections at around $2\theta = 19.98°$ and a weak shoulder at 21.95°. The two peaks are characteristic of PVA (Ricciardi, Auriemma, De Rosa, & Lauprêtre, 2004; Tang, Tian, & Hsu, 2015) On the other hand, there are two distinct peaks at 19^o and 22^o in the XRD diffractogram of PVA/Na-$Cell_4$;0kGy nanocomposite biofilms. These peaks are assigned for cellulose and their intensities slightly decrease upon irradiation with 20kGy. This may be attributed to that low dose of irradiation displayed very minor changes on the crystallinity of alkali cellulose. Our findings are consistent with Takacs et al. who observed slight changes in the crystallinity pattern at low irradiation dose and the emergence of cellulose II at high doses of irradiation (Takacs et al., 2000). However, it is stated that the alkali treatment of cellulose enhances the crystal structure depending on the concentration of NaOH (Kunusa, Isa, Laliyo, & Iyabu, 2018). This means that both the crystal and amorphous structure existed (Nishiyama, Kuga, & Okano, 2000).

3.5. Effect of alkaline cellulose on mechanical properties of the biofilms

Mechanical properties are critical factors in determining film workability (Vasile, 2018; Yadav & Chiu, 2019). Packaging materials must have reasonable tensile strength and mobility, as well as precision when acting as packing units (Wu, Farnood, O'Kelly, & Chen, 2014). In this context, the mechanical properties of the PVA/Na-Cell films were compared, Figure 4E-G. The stress/strain curve (Figure 4E) shows that the PVA film displayed inferior mechanical properties while PVA/Na-$Cell_4$ film achieves moderate elasticity (about 22.5 N) which is suitable for packaging under irradiation doses of 20kGy. Although irradiation increased the number of crosslinking points and thus increases the hardness, the unequal distribution of these points may induce the opposite effect. Thus, at a dose of 20 kGy, the maximum stress value for PVA/Na-$Cell_4$ was obtained. Furthermore, the values of elasticity modulus (Figure 4F) and elongation at break (Figure 4G) are maximum for PVA/Na-$Cell_4$ at the irradiation dose of 20 kGy. The results showed that the flexibility and durability of PVA/Na-$Cell_4$ film at a dose of 20 kGy are suitable for packaging applications.

3.6. Contact angle measurements

The water contact angle is important to determine whether the surface is hydrophobic or hydrophilic as an important feature for packaging materials (Abreu et al., 2015). Contact angle measurements were conducted for PVA/Na-$Cell_4$;0kGy, PVA/Na-$Cell_4$;20kGy, and PVA/Na-$Cell_4$/ECO;20kGy film surfaces over 10 seconds, as shown in Figure 5, and the results are summarized in Table 2C. Generally, the contact angle greater than 90^o reveals hydrophobic surface. The contact angle of pristine PVA films is about $6.3\pm0.4\ ^o$ according to Yang et al (Yang, Yoo, Lee, Kim, & Yeum, 2017) which indicates very high water solubility. However, PVA/Na-$Cell_4$;0kGy has a mean contact angle of 102.48^o which reflects the role of alkaline cellulose in improving the hydrophobicity of the biofilm. Additionally, Gamma irradiation appears to improve the contact angle of PVA/Na-$Cell_4$;20kGy to 133.66^o. However, the contact angle of the film fabricated with ECO is 140.62^o, indicating an increase in hydrophobicity. The films have high wettability resistance and are recommended as a packaging material.

(A)

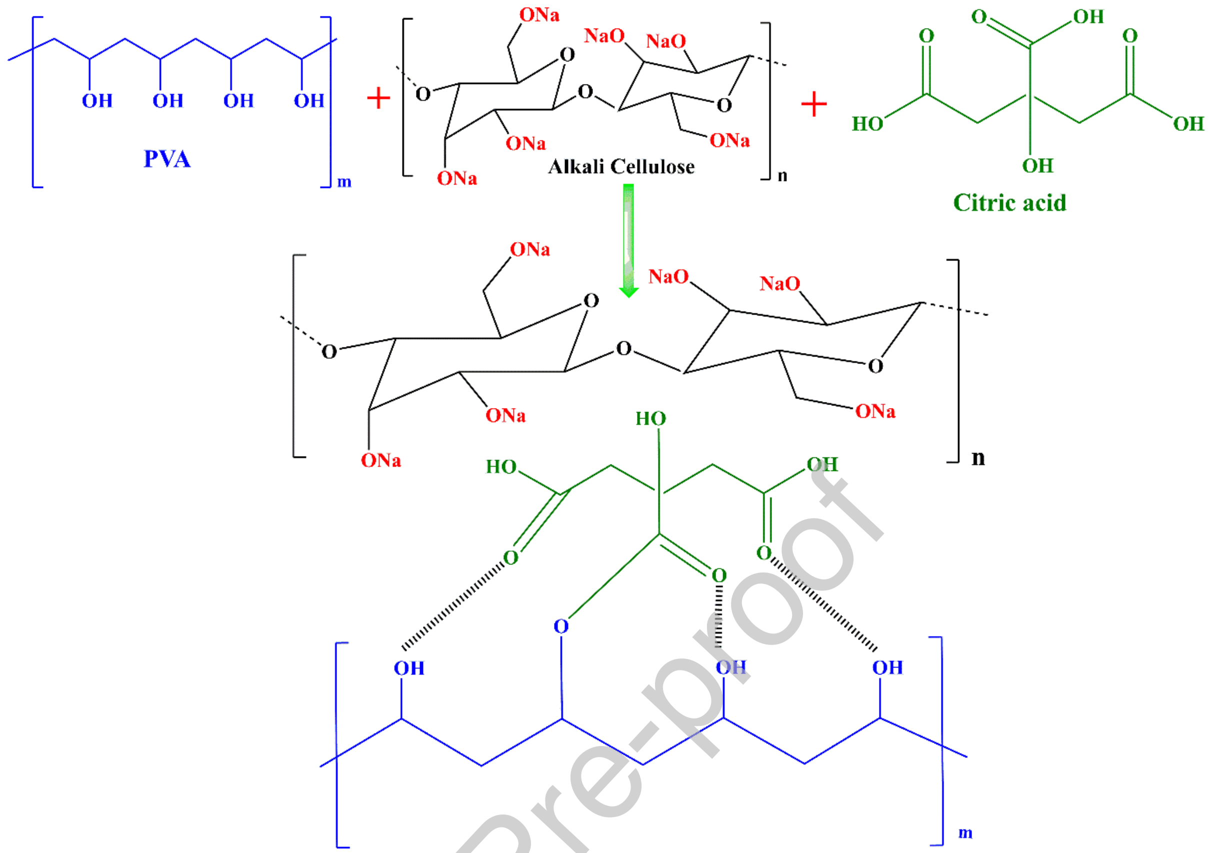

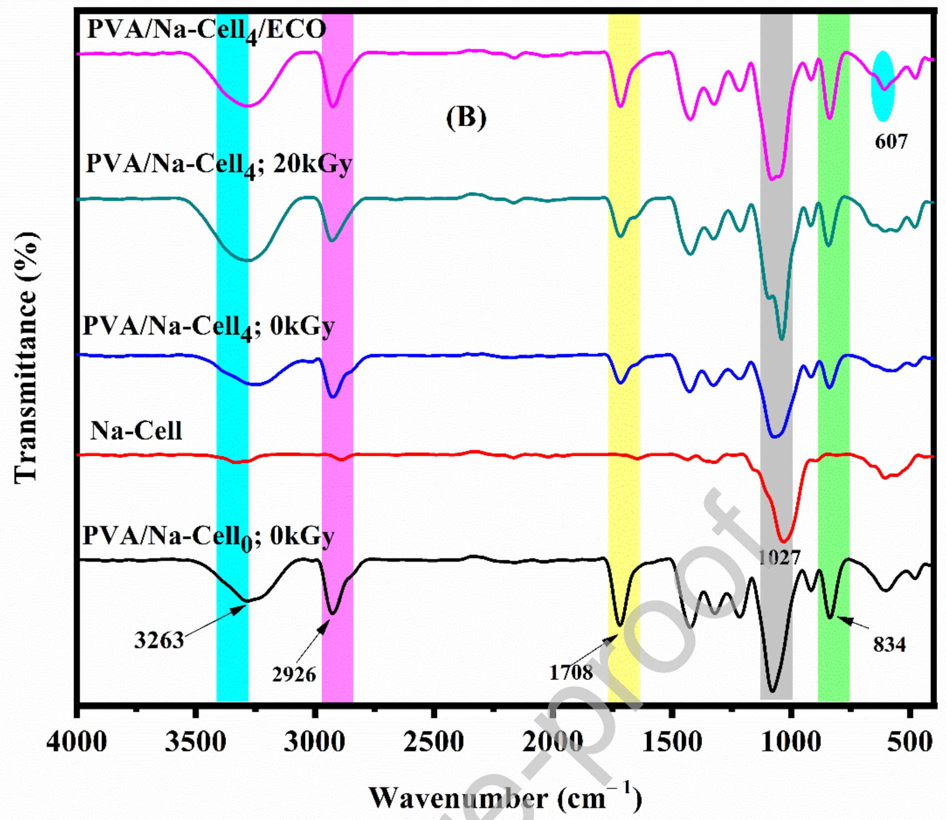

PVA/Na-Cell4/ECO
(B)
607
PVA/Na-Cell4; 20kGy
PVA/Na-Cell4; 0kGy
Na-Cell
PVA/Na-Cell0; 0kGy
1027
3263
2926
1708
834
Transmittance (%)
4000 3500 3000 2500 2000 1500 1000 500
Wavenumber (cm−1)

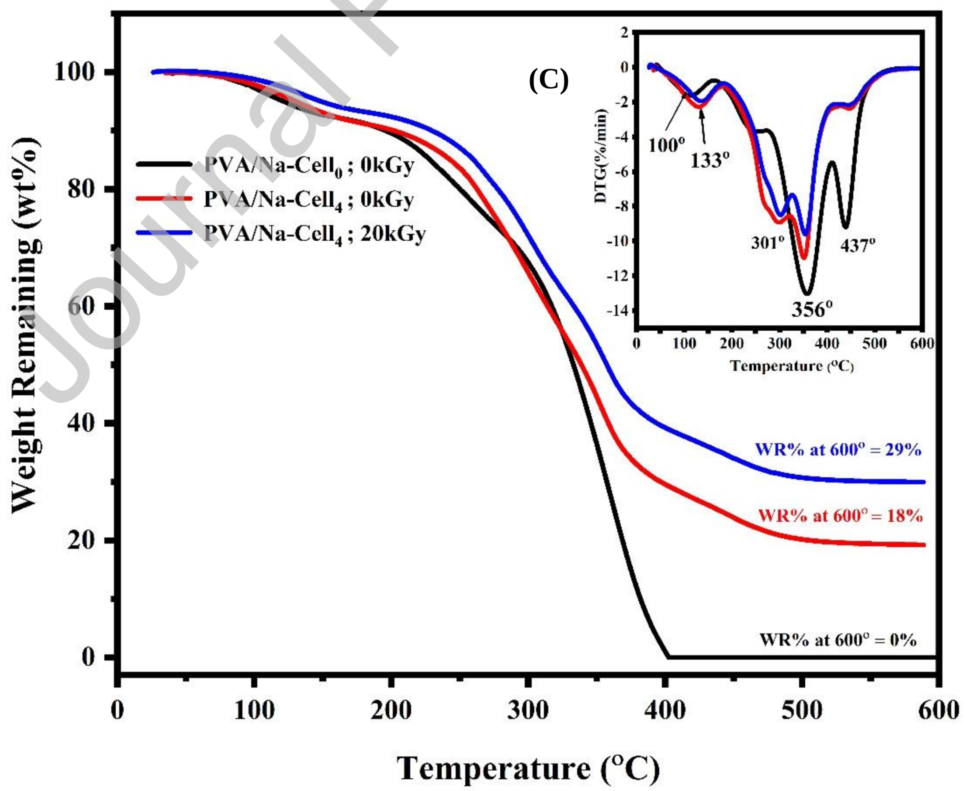

(C)
PVA/Na-Cell0 ; 0kGy
PVA/Na-Cell4 ; 0kGy
PVA/Na-Cell4 ; 20kGy
Weight Remaining (wt%)
Temperature (°C)
WR% at 600° = 29%
WR% at 600° = 18%
WR% at 600° = 0%
DTG(%/min)
100°
133°
301°
356°
437°
Temperature (°C)

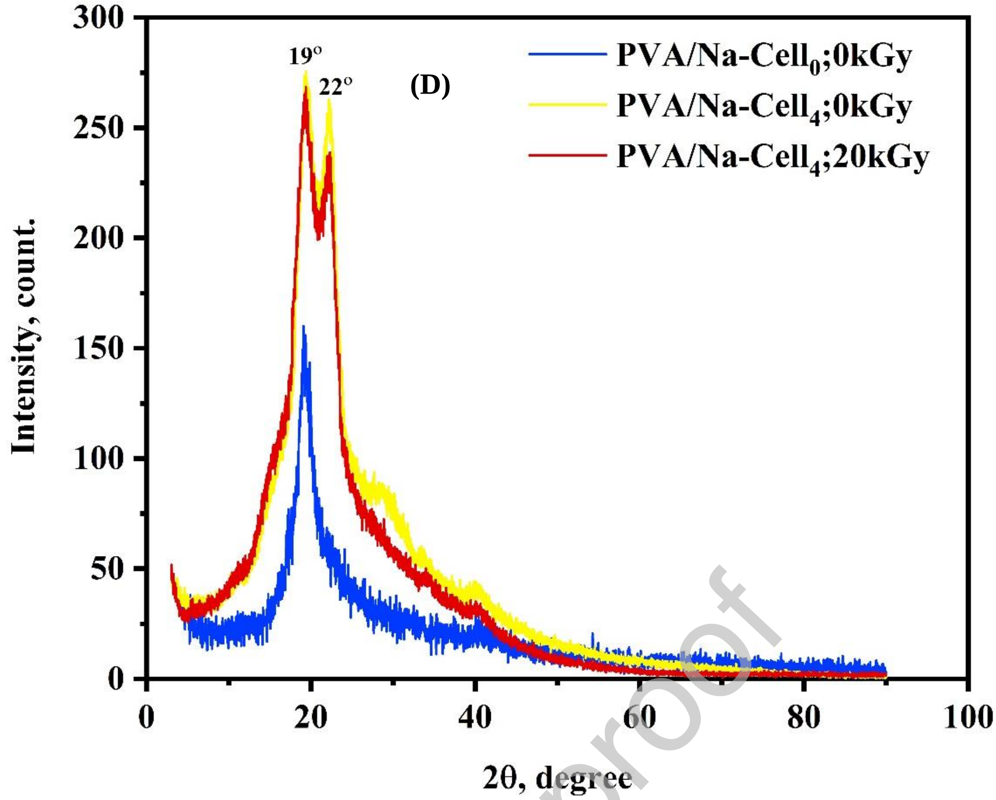

(D)
19°
22°
PVA/Na-Cell0;0kGy
PVA/Na-Cell4;0kGy
PVA/Na-Cell4;20kGy
Intensity, count.
2θ, degree

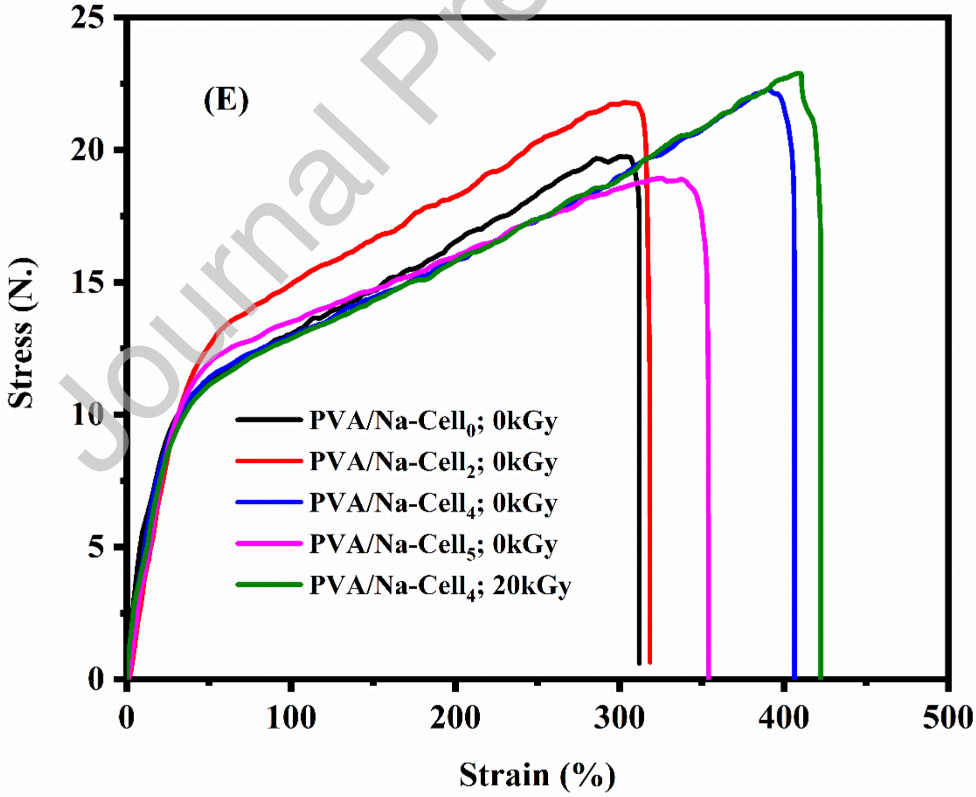

(E)
PVA/Na-Cell0; 0kGy
PVA/Na-Cell2; 0kGy
PVA/Na-Cell4; 0kGy
PVA/Na-Cell5; 0kGy
PVA/Na-Cell4; 20kGy
Stress (N.)
Strain (%)

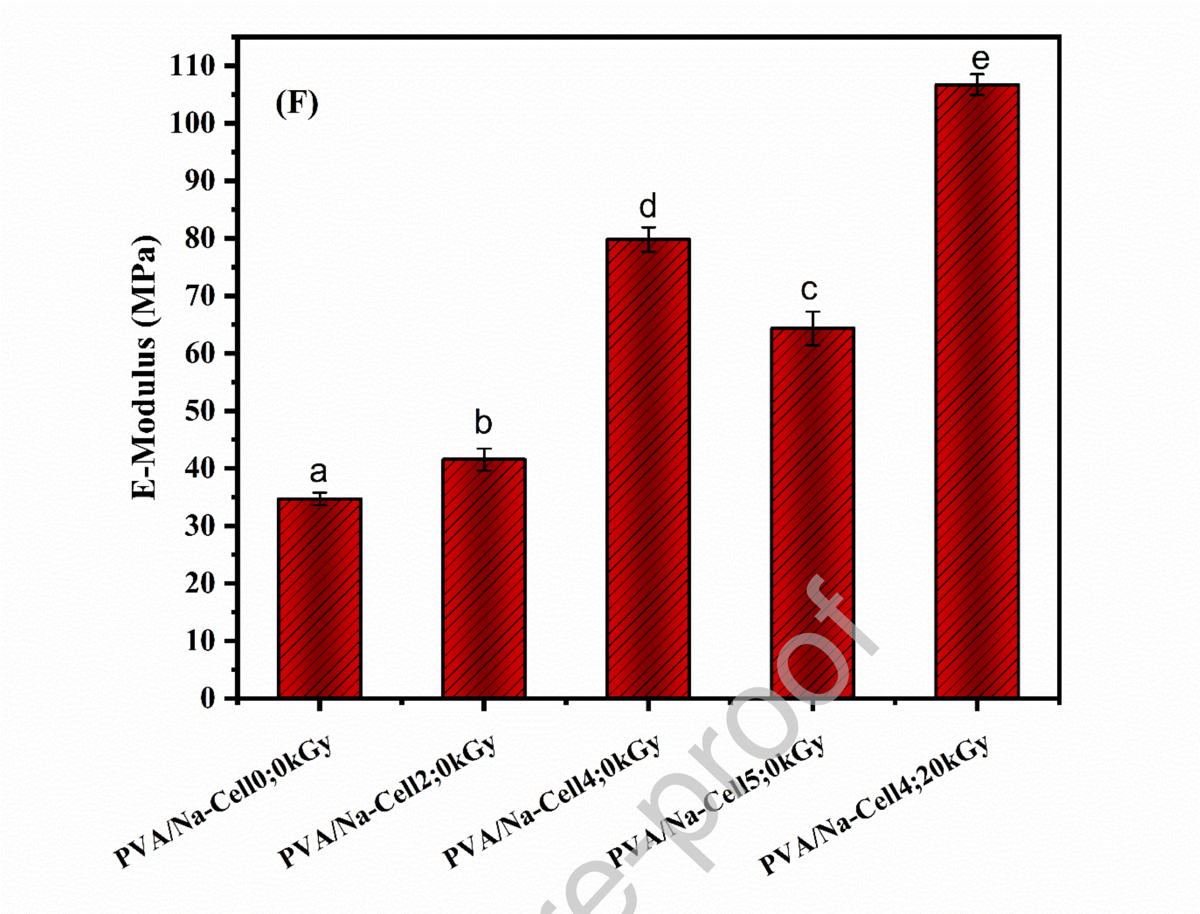
(F)
E-Modulus (MPa)
0
10
20
30
40
50
60
70
80
90
100
110
a
b
d
c
e
PVA/Na-Cell0;0kGy
PVA/Na-Cell2;0kGy
PVA/Na-Cell4;0kGy
PVA/Na-Cell5;0kGy
PVA/Na-Cell4;20kGy

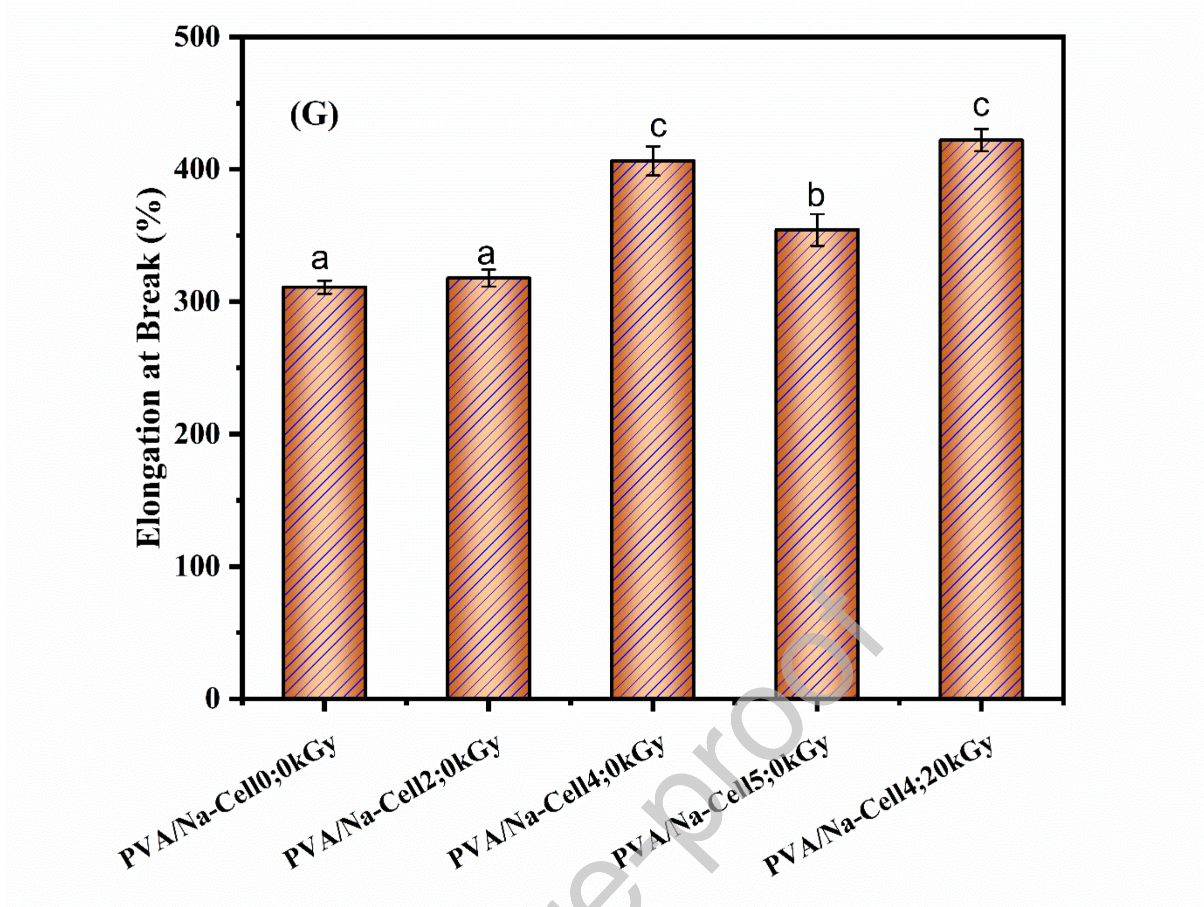

Figure 4: (A) the possible reaction mechanism for preparation of PVA/Na-Cell films; (B) FTIR spectra of PVA/Na-$Cell_0$;0kGy, Na-Cell, PVA/Na-$Cell_4$;0kGy, PVA/Na-$Cell_4$;20kGy, and PVA/Na-$Cell_4$/ECO;20kGy ; (C) TGA and DTA analysis ; (D) XRD diffraction patterns of PVA/Na-$Cell_4$;0kGy and PVA/Na-$Cell_4$; 20kGy; (E) Stress-Strain curve of PVA/Na-$Cell_x$;(F) E-Modulus (MPa) of PVA/Na-$Cell_x$ and (G) Elongation at break (%) of PVA/Na-$Cell_x$; *The values are the means ± SD, n=5. Bars with different letters are significantly different at P<0.05.*

Table 2B: Thermal characteristics of PVA/Na-$Cell_0$;0kGy, PVA/Na-$Cell_4$;0kGy, PVA/Na-$Cell_4$;20kGy

Sample	Weight Loss (%) at (100-133) ^{o}C	Weight Loss (%) at 356^{o}C	Total weight loss (%) at 600^{o}C
PVA/Na-$Cell_0$;0kGy	3-7wt%	70wt%	100wt%
PVA/Na-$Cell_4$;0kGy	2-5wt%	63wt%	82wt%
PVA/Na-$Cell_4$;20kGy	1-4wt%	49wt%	71wt%

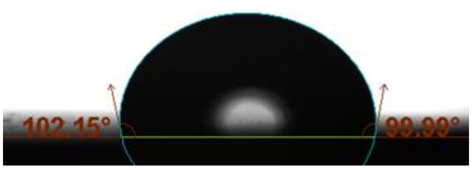

PVA/Na-$Cell_4$;0kGy

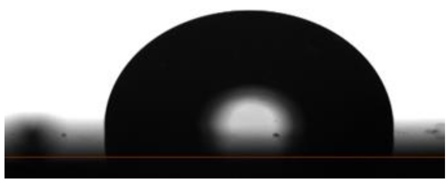

PVA/Na-$Cell_4$;20kGy

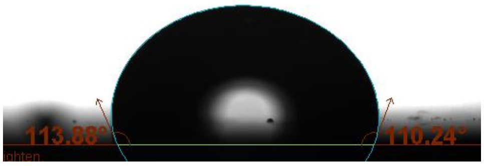

PVA/Na-Cell$_4$/ECO;20kGy

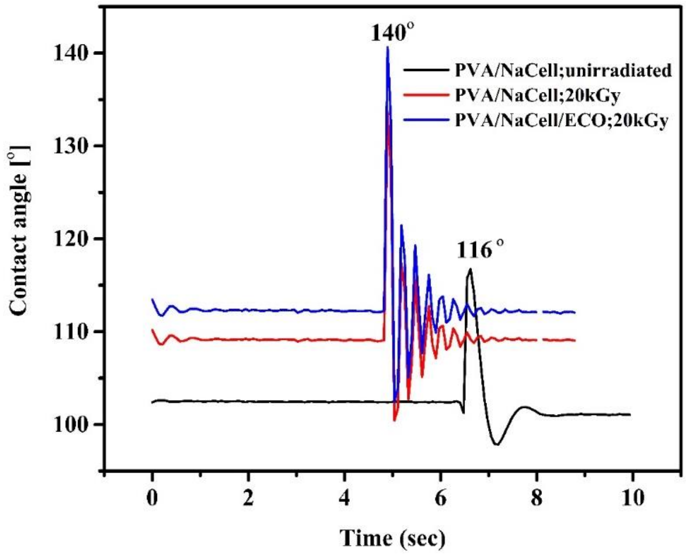

Figure 5: contact angel analysis of PVA/Na-Cell$_4$;0kGy, PVA/Na-Cell$_4$;20kGy, and PVA/Na-Cell$_4$/ECO;20kGy films.

Table 2C: Contact angle parameters PVA/Na-Cell$_4$;0kGy, PVA/Na-Cell$_4$;20kGy, and PVA/Na-Cell$_4$/ECO;20kGy films

Sample	CA left, [°]	CA right, [°]	CA mean, [°]	ST, [mN/m]	Height, [mm]	Area, [mm^2]
PVA/Na-Cell$_4$;0kGy	104.63^a±1.1	100.32^a±0.99	102.48^a±1.03	20.03^a±0.8	2.17^a±0.01	28.32^a±0.2
PVA/Na-Cell$_4$;20kGy	131.30^b±2.1	136.02^b±1.23	133.66^b±1.67	118.48^b±2.9	2.39^b±0.02	35.07^b±0.3
PVA/Na-Cell$_4$/ECO;20kGy	137.94^c±2.2	143.30^c±2.06	140.62^c±2.05	118.48^b±2.8	2.45^c±0.02	36.15^c±0.2

[*]The values are the means ± SD, n=3 inside each column with different letters are significantly different at P<0.05, Duncan's test.

3.7. Antimicrobial Activity of PVA/NaCell./ECO Films

The antimicrobial activity of PVA/Na-Cell$_4$/ECO;20kGy films containing different concentrations of ECO was investigated against Gram-positive bacteria *(Bacillus Subtilis & Staph.aureus)*, Gram-negative bacteria (*Escherichia coli & Pseudomonas aeruginosa)* and fungi (*Candida albicans & Aspergillus niger)* as shown in Figure 6. The inhibition zones are tabulated in Table 3. It is clear that PVA/Na-Cell$_4$/ECO;20kGy films exhibited robust antibacterial properties against all pathogenic species tested except *Aspergillus niger* fungus. As the concentration of ECO was increased, the inhibition effect against all the tested microbes was enhanced. The antimicrobial investigation revealed that the films fabricated with ECO displayed an effective antimicrobial activity against different gram-negative and gram-positive bacteria. The antimicrobial activity of all the prepared films fabricated with ECO proportionally increases with the concentration of ECO. This finding confirmed the potent antimicrobial action of ECO (Nuñez & D'Aquino, 2012).

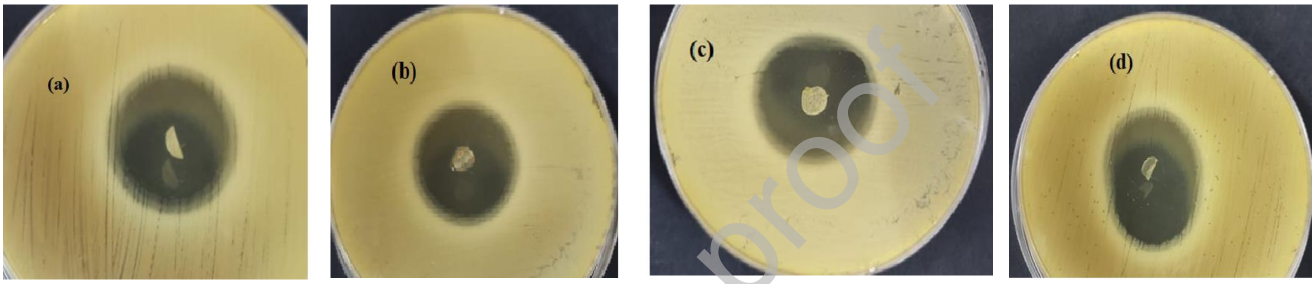

Candida albicans (ATCC 10221)

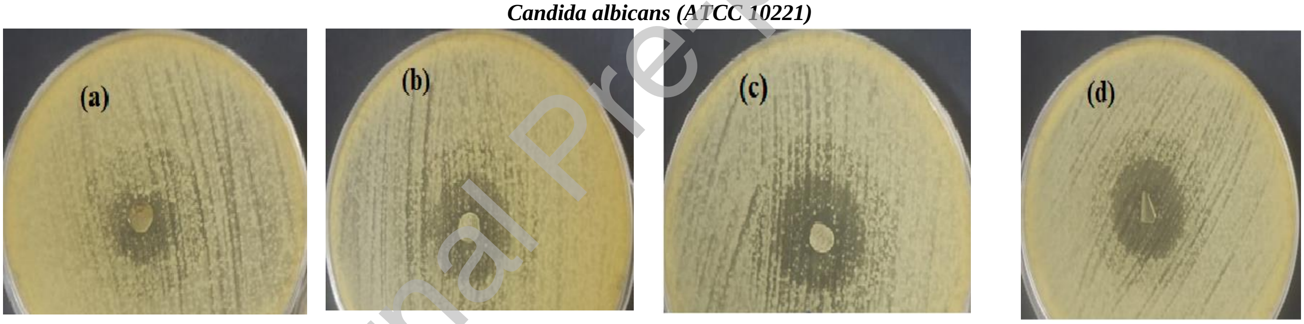

Escherichia coli (ATCC 8739)

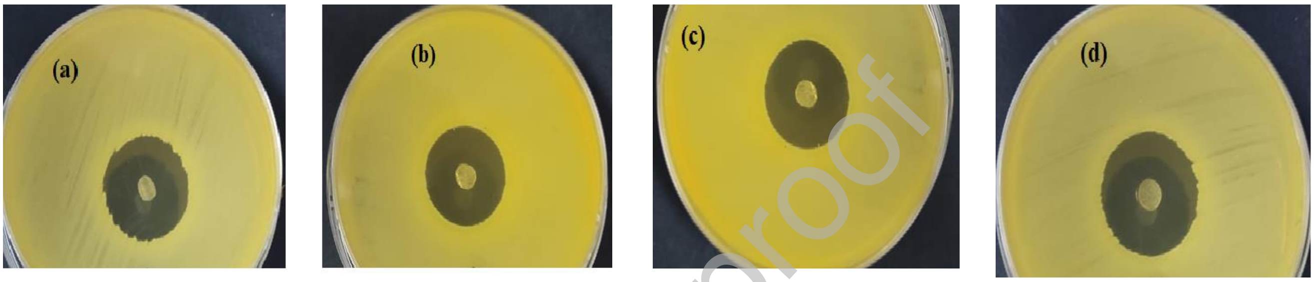

Staph.aureus (ATCC 6538)

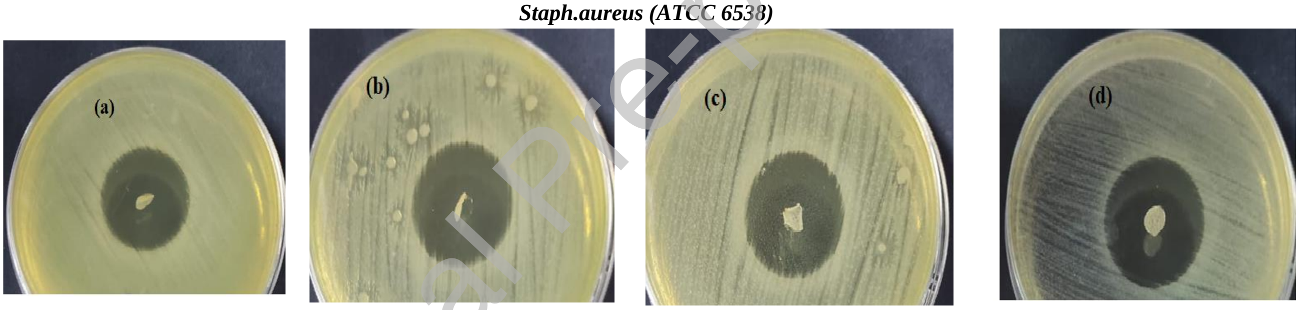

Pseudomonas aeruginosa (ATCC 90274)

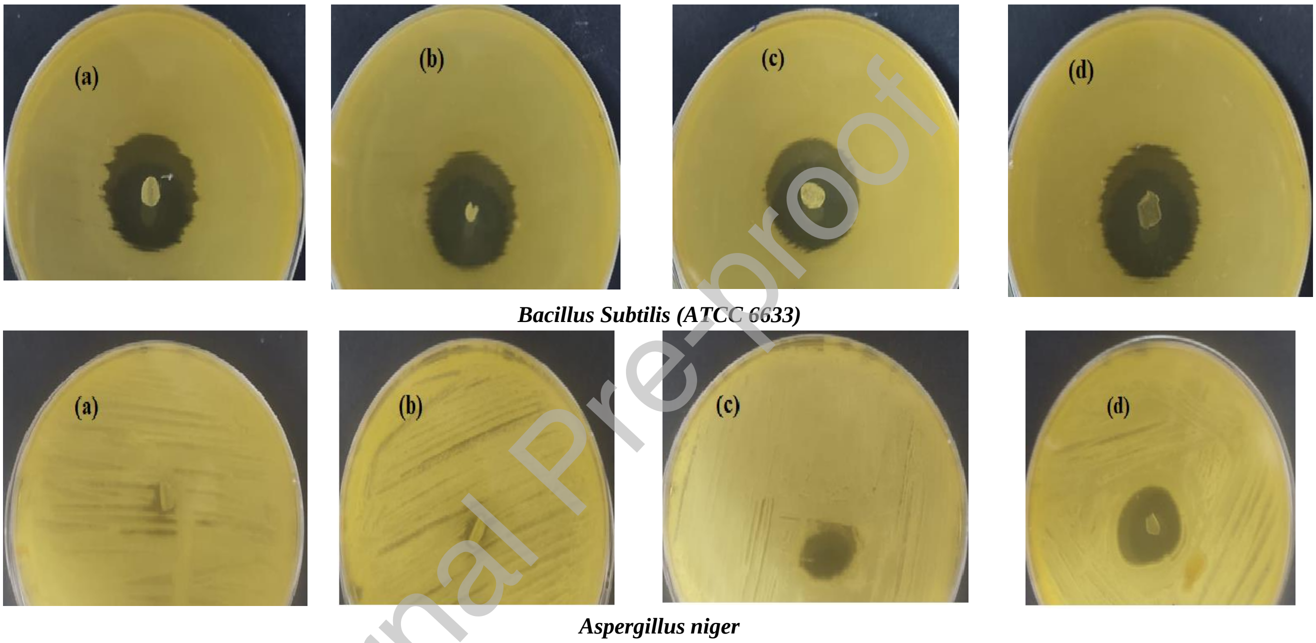

Figure (6): Antimicrobial activity of PVA/Na-Cell$_4$/ECO;20kGy at different ECO concentration (a) 25µmL; (b)50µmL; (c) 75µmL and (d)100µmL

Table (3): Antimicrobial activity data of PVA/Na-$Cell_4$/ECO;20kGy films at different concentrations of ECO

Sample / Pathogenic Microorganism	ECO concentration, µmL			
	25	**50**	**75**	**100**
	inhibition zoon (mm)			
Bacillus Subtilis (ATCC 6633)	25	26	26	29
Staph.aureus (ATCC 6538)	25	25	27	29
Escherichia coli (ATCC 8739)	16	21	22	25
Pseudomonas aeruginosa (ATCC 90274)	26	27	28	34
Candida albicans (ATCC 10221	27	28	29	30
Aspergillus niger	NA	NA	15	21

Conclusions:

Novel cellulose-based biofilms with potent antimicrobial activity were prepared via multi-step preparations aided with the AFM data (topography, height and roughness) to select the optimized samples for the next preparation step. Initially polyvinyl alcohol/alkaline cellulose films were prepared by physical crosslinking through solvent-casting method. The prepared films were characterized by the AFM to investigate the effect of alkaline cellulose on the surface features of the biofilms. The outcomes revealed that the optimum membrane was PVA/Na-$Cell_4$. This membrane was exposed to three irradiation doses and the membranes obtained at this step were also evaluated by the AFM where the selected membrane was the one exposed to 20kGy dose. The hydrophobicity and water resistance of the membranes was verified via the contact angle measurements. Some selected samples were characterized by TGA and XRD analyses in order to investigate the effect of both alkaline cellulose and irradiation on their thermal stability and crystallographic properties. The data showed that both the alkaline cellulose and an optimized irradiation dose improved the workability of the PVA membrane.

Ethical approval

Not applicable.

Consent to participate

Not applicable.

Consent to publish

All authors approved the publication.

Funding

Not applicable.

Availability of data and materials

The authors declare that all data supporting the findings and materials of this study are available within the paper.

CRediT authorship contribution statement

Asmaa Sayed was responsible for preparation Software, validation, data curation and data interpretation. Manar Abdel-raouf was responsible for analysis, the AFM investigation and data interpretation, writing- revising, and editing manuscript. Gehan Safwat was responsible for the conception and design, analysis and data interpretation. Ghada A. Mahmoud was responsible for testing, data acquisition, writing- revising, and editing. All authors read, revised, and approved the final manuscript.

Declaration of competing interest

The authors declare no known competing financial interests or personal relationships that could have appeared to influence the work reported in this paper.

References

Abreu, A. S., Oliveira, M., de Sá, A., Rodrigues, R. M., Cerqueira, M. A., Vicente, A. A., & Machado, A. (2015). Antimicrobial nanostructured starch based films for packaging. *Carbohydrate Polymers*, 129, 127-134.

Al-qudah, Y. H., Mahmoud, G. A., & Abdel Khalek, M. (2014). Radiation crosslinked poly (vinyl alcohol)/acrylic acid copolymer for removal of heavy metal ions from aqueous solutions. *Journal of Radiation Research and Applied Sciences*, 7(2), 135-145.

Al-Qudaha, Y. H., Hegazy, N., Mahmoud, G. A., & Hegazyb, E. (2022). Bio-based composite reinforced with peanut shells prepared by ionizing radiation for removal of Ni2+ and Co2+ ions. *DESALINATION AND WATER TREATMENT*, 252, 177-185.

Andrade, M. S., Ishikawa, O. H., Costa, R. S., Seixas, M. V. S., Rodrigues, R. C. L. B., & Moura, E. A. B. (2022). Development of sustainable food packaging material based on biodegradable polymer reinforced with cellulose nanocrystals. *Food Packaging and Shelf Life*, 31, 100807., https://doi.org/10.1016/j.fpsl.2021.100807

Arrieta, M. P., Fortunati, E., Dominici, F., Rayón, E., López, J., & Kenny, J. M. (2014). Multifunctional PLA–PHB/cellulose nanocrystal films: processing, structural and thermal properties. *Carbohydrate Polymers*, 107, 16-24.

Azman, N. A. M. (2022). *Active biocomposite packaging films: Compatibility of carrageenan with cellulose nanofiber from empty fruit bunches*. In *Industrial Applications of Nanocellulose and Its Nanocomposites* (pp. 311-326): Elsevier

Bahrami, A., & Fattahi, R. (2021). Biodegradable carboxymethyl cellulose–polyvinyl alcohol composite incorporated with Glycyrrhiza Glabra L. essential oil: Physicochemical and antibacterial features. *Food Science & Nutrition*, 9(9), 4974-4985.

Baranwal, J., Barse, B., Fais, A., Delogu, G. L., & Kumar, A. (2022). Biopolymer: A Sustainable Material for Food and Medical Applications. Polymers (Basel), 14, 983, https://doi.org/10.3390/polym14050983. https://www.mdpi.com/journal/polymers.

Boufi, S., González, I., Delgado-Aguilar, M., Tarres, Q., Pèlach, M. À., & Mutje, P. (2016). Nanofibrillated cellulose as an additive in papermaking process: A review. *Carbohydrate Polymers*, 154, 151-166.

Campiglio, C. E., Ponzini, S., De Stefano, P., Ortoleva, G., Vignati, L., & Draghi, L. (2020). Cross-linking optimization for electrospun gelatin: Challenge of preserving fiber topography. *Polymers*, 12(11), 2472.

Chu, Y., Xu, T., Gao, C., Liu, X., Zhang, N., Feng, X., Tang, X. (2019). Evaluations of physicochemical and biological properties of pullulan-based films incorporated with cinnamon essential oil and Tween 80. *International journal of biological macromolecules*, 122, 388-394.

Das, A., Ringu, T., Ghosh, S., & Pramanik, N. (2022). A comprehensive review on recent advances in preparation, physicochemical characterization, and bioengineering applications of biopolymers. *Polymer Bulletin*, 1-66. https://doi.org/10.1007/s00289-022-04443-4

El Miri, N., El Achaby, M., Fihri, A., Larzek, M., Zahouily, M., Abdelouahdi, K., Solhy, A. (2016). Synergistic effect of cellulose nanocrystals/graphene oxide nanosheets as functional hybrid nanofiller for enhancing properties of PVA nanocomposites. *Carbohydrate Polymers*, 137, 239-248.

Helanto, K. E., Matikainen, L., Talja, R., & Rojas, O. J. (2019). Bio-based polymers for sustainable packaging and biobarriers: A critical review. *BioResources*, 14(2), 4902-4951.

Kuai, L., Liu, F., Chiou, B.-S., Avena-Bustillos, R. J., McHugh, T. H., & Zhong, F. (2021). Controlled release of antioxidants from active food packaging: A review. *Food Hydrocolloids*, 120, 106992. https://doi.org/10.1016/j.foodhyd.2021.106992

Kunusa, W. R., Isa, I., Laliyo, L. A., & Iyabu, H. (2018). FTIR, XRD and SEM analysis of microcrystalline cellulose (MCC) fibers from corncorbs in alkaline treatment. *Journal of Physics: Conference Series* (Vol. 1028, p. 012199): IOP Publishing.

Liu, Y., Ahmed, S., Sameen, D. E., Wang, Y., Lu, R., Dai, J.,Qin, W. (2021). A review of cellulose and its derivatives in biopolymer-based for food packaging application. *Trends in Food Science & Technology*, 112, 532-546.

Luesuwan, S., Naradisorn, M., Shiekh, K. A., Rachtanapun, P., & Tongdeesoontorn, W. (2021). Effect of active packaging material fortified with clove essential oil on fungal growth and post-harvest quality changes in table grape during cold storage. *Polymers*, 13(19), 3445.

Magaldi, S., Mata-Essayag, S., De Capriles, C. H., Pérez, C., Colella, M., Olaizola, C., & Ontiveros, Y. (2004). Well diffusion for antifungal susceptibility testing. *International journal of infectious diseases*, 8(1), 39-45.

Mane, S., Ponrathnam, S., & Chavan, N. (2015). Effect of chemical cross-linking on properties of polymer microbeads: a review. *Can Chem Trans*, 3(4), 473-485.

Miranda, C. S., Ferreira, M. S., Magalhães, M. T., Bispo, A. P. G., Oliveira, J. C., Silva, J. B., & José, N. M. (2015). Starch-based films plasticized with glycerol and lignin from piassava fiber reinforced with nanocrystals from eucalyptus. *Materials Today: Proceedings*, 2(1), 134-140.

Mulla, M., Ahmed, J., Al-Attar, H., Castro-Aguirre, E., Arfat, Y. A., & Auras, R. (2017). Antimicrobial efficacy of clove essential oil infused into chemically modified LLDPE film for chicken meat packaging. *Food Control*, 73, 663-671.

Nada, H. G., Mohsen, R., Zaki, M. E., & Aly, A. A. (2022). Evaluation of chemical composition, antioxidant, antibiofilm and antibacterial potency of essential oil extracted from gamma irradiated clove (Eugenia caryophyllata) buds. *Journal of Food Measurement and Characterization*, 16(1), 673-686.

Nisar, T., Wang, Z.-C., Yang, X., Tian, Y., Iqbal, M., & Guo, Y. (2018). Characterization of citrus pectin films integrated with clove bud essential oil: Physical, thermal, barrier, antioxidant and antibacterial properties. *International journal of biological macromolecules*, 106, 670-680.

Nishiyama, Y., Kuga, S., & Okano, T. (2000). Mechanism of mercerization revealed by X-ray diffraction. *Journal of wood science*, 46(6), 452-457.

Nordin, N., Othman, S., Kadir, R., & Rashid, S. (2018). Mechanical and thermal properties of starch films reinforced with microcellulose fibres. *Food Research*, 2, 555-563.

Nuñez, L., & D'Aquino, M. (2012). Microbicide activity of clove essential oil (Eugenia caryophyllata). *Brazilian journal of microbiology*, 43, 1255-1260.

Othman, N., Azahari, N. A., & Ismail, H. (2011). Thermal properties of polyvinyl alcohol (PVOH)/corn starch blend film. *Malaysian Polymer Journal*, 6(6), 147-154.

Ricciardi, R., Auriemma, F., De Rosa, C., & Lauprêtre, F. (2004). X-ray diffraction analysis of poly (vinyl alcohol) hydrogels, obtained by freezing and thawing techniques. *Macromolecules*, 37(5), 1921-1927.

Sayed, A., Hany, F., Abdel-Raouf, M. E.-S., & Mahmoud, G. A. (2022). Gamma irradiation synthesis of pectin- based biohydrogels for removal of lead cations from simulated solutions. *Journal of Polymer Research*, 29(9), 372.

Sayed, A., Mahmoud, G. A., Said, H., & Diab, A. A. (2022). Characterization and optimization of magnetic Gum-PVP/SiO2 nanocomposite hydrogel for removal of contaminated dyes. *Materials Chemistry and Physics*, 280, 125731. https://doi.org/10.1016/j.matchemphys.2022.125731

Sayed, A., Mohamed, M. M., Abdel-raouf, M. E.-S., & Mahmoud, G. A. (2022). Radiation Synthesis of Green Nanoarchitectonics of Guar Gum-Pectin/Polyacrylamide/Zinc Oxide Superabsorbent Hydrogel for Sustainable Agriculture. *Journal of Inorganic and Organometallic Polymers and Materials*, 1-16. https://doi.org/10.21203/rs.3.rs-1895268/v1

Sayed, A., Yasser, M., Abdel-raouf, M. E.-s., & Mohsen, R. (2022). Green starch/graphene oxide hydrogel nanocomposites for sustained release applications. *Chemical Papers*, 76(8), 5119-5132.

Schoukens, G., Breen, C., Baschetti, M. G., Elegir, G., Vähä-Nissi, M., Liu, Q.,Simon, P. (2014). Complex packaging structures based on wood derived products: Actual and future possibilities for 1-way food packages. *Journal of Materials Science Research,* 3(4), 58.

Sharma, S., Barkauskaite, S., Duffy, B., Jaiswal, A. K., & Jaiswal, S. (2020). Characterization and antimicrobial activity of biodegradable active packaging enriched with clove and thyme essential oil for food packaging application. *Foods*, 9(8), 1117.

Stadler, F. J., & García-Peñas, A. (2022). Water-Soluble and-Insoluble Polymers and Biopolymers for Biomedical, Environmental, and Biological Applications. (Vol. 14, p. 2386): MDPI.

Suganthi, S., Vignesh, S., Kalyana Sundar, J., & Raj, V. (2020). Fabrication of PVA polymer films with improved antibacterial activity by fine-tuning via organic acids for food packaging applications. *Applied Water Science,* 10(4), 1-11.

Tajeddin, B. (2014). Cellulose-based polymers for packaging applications. *Lignocellulosic Polymer Composites,* 477-498.

Takacs, E., Wojnarovits, L., Földváry, C., Hargittai, P., Borsa, J., & Sajo, I. (2000). Effect of combined gamma-irradiation and alkali treatment on cotton–cellulose. *Radiation Physics and Chemistry,* 57(3-6), 399-403.

Tang, C.-M., Tian, Y.-H., & Hsu, S.-H. (2015). Poly (vinyl alcohol) nanocomposites reinforced with bamboo charcoal nanoparticles: mineralization behavior and characterization. *Materials,* 8(8), 4895-4911.

Tu, H., Li, X., Liu, Y., Luo, L., Duan, B., & Zhang, R. (2022). Recent progress in regenerated cellulose-based fibers from alkali/urea system via spinning process. *Carbohydrate Polymers,* 296, 119942.

Vasile, C. (2018). Polymeric nanocomposites and nanocoatings for food packaging: A review. *Materials,* 11(10), 1834.

Wu, T., Farnood, R., O'Kelly, K., & Chen, B. (2014). Mechanical behavior of transparent nanofibrillar cellulose–chitosan nanocomposite films in dry and wet conditions. *journal of the mechanical behavior of biomedical materials,* 32, 279-286.

Xia, G., Ji, X., Xu, Z., & Ji, X. (2022). Transparent cellulose-based bio-hybrid films with enhanced anti-ultraviolet, antioxidant and antibacterial performance. *Carbohydrate Polymers,* 298, 120118.

Yadav, M., & Chiu, F.-C. (2019). Cellulose nanocrystals reinforced κ-carrageenan based UV resistant transparent bionanocomposite films for sustainable packaging applications. *Carbohydrate Polymers,* 211, 181-194.

Yang, S. B., Yoo, S. H., Lee, J. S., Kim, J. W., & Yeum, J. H. (2017). Surface properties of a novel poly (vinyl alcohol) film prepared by heterogeneous saponification of poly (vinyl acetate) film. *Polymers*, 9(10), 493.

Yuvaraj, D., Iyyappan, J., Gnanasekaran, R., Ishwarya, G., Harshini, R., Dhithya, V., Gomathi, K. (2021). Advances in bio food packaging–An overview. *Heliyon,* 7(9), e07998.

Conflict of interest

Dear Editor-in-chief:

Carbohydrate polymer technologies and applications:

The authors declare that they have no known competing financial interests or personal relationships that could have appeared to influence the work entitled:

Alkali-cellulose/ Polyvinyl alcohol biofilms fabricated with essential clove oil as a novel scented antimicrobial packaging material

Asmaa Sayed[1], Gehan Safwat[2], Manar Abdel-raouf *[3]and Ghada A. Mahmoud[1]

[1]Polymer Chemistry Department, National Center for Radiation Research and Technology, Egyptian Atomic Energy Authority, Cairo, Egypt.
[2]Faculty of Biotechnology, October University for Modern Sciences and Arts (MSA) Egypt.
[3]Egyptian Petroleum Research Institute, 1Ahmed Elzomor Street, 11727, Nasr city, Cairo, Egypt

*Email corresponding author: drmanar770@yahoo.com, Tel.:202-22745902

Graphical Abstract